Information Content in O[1s] K-edge X-ray Emission Spectroscopy of Liquid Water

Michael Odelius*

FYSIKUM, Stockholm University, Albanova, S-106 91 Stockholm, Sweden

Received: April 3, 2009; Revised Manuscript Received: June 2, 2009

Does the fine-structure in oxygen K-edge X-ray emission (Fuchs et al. *Phys. Rev. Lett.* **2008**, *100*, 027801) imply that liquid water is a two-component mixture or is it the signature of a transient OH species arising in the core-excitation process? As with the interpretation of the X-ray absorption spectrum of liquid water, this question is also intensely discussed in the water and X-ray spectroscopy communities. X-ray emission is an independent probe of the electronic structure yielding complementary information on hydrogen bonding in liquid water. In this study, the angular anisotropy in the resonant inelastic soft X-ray scattering (resonant X-ray emission (XE)) spectrum of liquid water is simulated on the basis of ab initio molecular dynamics simulations to allow for direct comparison to recent experimental data (Forsberg et al. *Phys. Rev. B* **2009**, *79*, 132203). Theoretical simulations unequivocally show that the difference in angular anisotropy in the water lone-pair features is related to their fundamentally different origin. The high emission-energy peak is primarily due to the contribution from the out-of-plane ($1b_1$) lone-pair in intact water molecules. On the other hand, the low emission-energy lone-pair peak originates from the bonding ($3a_1$) state and is assigned to a transient OH species formed by ultrafast (<10 fs) photodissociation. The information in the XE spectrum on the structure of liquid water is limited and buried in features arising from excited state dynamics. In combination with available experimental data, the theoretical simulations settle a rising debate on the interpretation of resonant and nonresonant XE spectra of liquid water and there are strong implications for the XE spectroscopy of hydrogen-bonded liquids. The simulations show that the fine-structure in the XE spectrum of liquid water can be explained simply in terms of present day ab initio molecular dynamics simulations.

1. Introduction

X-ray emission (XE) spectroscopy[1] is a unique tool for obtaining element-specific electronic information in complex systems. It is a valuable complement to other experimental probes of the electronic structure in the condensed phase. After core-excitation of a specific element, in this case oxygen, decay of the O[1s] core-hole gives rise to emission of a X-ray photon when a valence electron falls down to fill the core-hole. Thus, the XE process can be viewed as a local projection of the valence electronic structure depicting the local density of states on the core-excited atom. Resonant X-ray emission, or more accurately resonant inelastic soft X-ray scattering (RIXS),[1] contains additional information. In RIXS, each region of the X-ray absorption spectrum, and its associated intermediate core-excited states, results in a specific projection of the local density of states. Hence, RIXS contains information not only on the configurational selectivity of the core-excitation but also processes occurring in the intermediate state as well as the overlap between the initial, final, and intermediate electronic states.

The specific aim of the present study is to provide a detailed molecular interpretation of the recently published angular anisotropy in RIXS at the oxygen K-edge (O[1s]) of liquid water.[2] The experimental data could be improved both in terms of signal-to-noise ratio and the extension of the excitation energies probed, but the data from the existing experiments are already very informative. I show that extended studies of angular anisotropy in RIXS could be a crucial piece of evidence in understanding X-ray emission in liquid water.[3−11] Furthermore, a RIXS map over different excitation energies would provide unique information on the character of the X-ray absorption (XA) spectrum. The controversial claims about the hydrogen (H-)bonding in liquid water from the interpretation of X-ray absorption data[12,13] were partly based on theoretical calculations. Alternative theoretical methods have been used to reinterpret the experimental data[14,15] but there is no consensus on the applicability of these methods.[13−19] Additional electronic information on the XA spectrum of liquid water is essential to evaluate the approximations employed in the models used to simulate XA spectra.

The recent experimental development of liquid cells and liquid jets has enabled studies of XE and RIXS in the liquid phase and in particular on water and other H-bonded liquids.[3−9,20,21] This method is relatively new in the field of molecular liquids and so it is desirable to clarify its information content and to determine how to extract useful information from the data. In the literature, two incompatible classes of interpretations of X-ray emission spectra of H-bonded liquids are advocated.

On one hand, the fine-structure in the XE spectrum has been employed to unravel amazingly detailed information on specific molecular structures in liquid water, alcohols, and alcohol-water mixtures.[3,4,9,10,20,21] For liquid water at least, these conclusions are at odds with state-of-the-art molecular dynamics (MD) simulations.[9]

Conversely, there are experimental and theoretical XE studies of water[2,5−7,11,22] from which an alternative interpretation of the XE fine-structure of H-bonded liquids can be derived. Because of the evolution in the excited state during the finite lifetime of the core-hole, the fine-structure components are not directly related to the ground-state structural or electronic configuration.

* E-mail: odelius@fysik.su.se.

10.1021/jp903096k CCC: $40.75

Experimentally derived arguments[6,7] for the presence of a transient OH species arising from photodissociation are essentially in agreement with XE spectra derived from ab initio MD simulations.[5,11,22]

2. Theoretical Basis

The RIXS process can be described by the Kramer−Heisenberg formula

$$F(\omega,\omega') = \sum_f \left[\sum_m \frac{\langle f|D|m\rangle\langle m|D|g\rangle}{E_g + \omega - E_m - i\Gamma_m}\right]^2 \delta(E_g + \omega - E_f - \omega') \quad (1)$$

which expresses the transition from the initial (electronic ground) state, g, via the intermediate (core-excited) states, m, to the final (valence-excited) states, f.[23−25]

The weights of the different possible pathways depend on the absorption energy, ω, and emission energy, ω', with respect to the energies of the states, E_g, E_m, and E_f. The transition dipole operator, D, gives the absorption and emission transition moments and Γ_m describes the rapid decay of the intermediate states. (The core-excited states are directly detected in near-edge X-ray absorption spectroscopy.)

A time-dependent representation[23,25,26] can be used to derive the scattering amplitude in eq 1 from the evolution of the wave function during core-excitation and the lifetime of the core-hole. However, in the present framework the RIXS process is derived from stationary electronic states along classical trajectories in the core-excited state.

Equation 2 shows the dependence of the scattering intensity on the angle (θ) between the polarization of the incoming X-rays and the direction from the sample to the detector in the experimental setup[3]

$$I(\theta) = I_0\left[1 + R\left(\frac{3}{2}\sin^2\theta - 1\right)\right] \qquad R = \frac{1}{5}(\cos^2\varphi - 1) \quad (2)$$

The factor R in eq 2 describes the dependence of the intensity on the relative orientation of the XA and XE transition moments in the inelastic X-ray scattering process.[24,25,27] It depends on the angle ϕ between the XA and XE transition moments. In this way, the random distribution of the orientation of the water molecules in the liquid is included in the calculations.

The excitation energy dependence in RIXS spectroscopy arises from the nature of the intermediate states and can be due to any combination of four principally different mechanisms: (a) the contributions from the different configurations of water molecules at each particular X-ray absorption energy, (b) differences in the dynamic response to the core-excited state potentials (c) overlap effects due to the symmetry of the absorption and emission transition moments, and (d) quantum interference effects between the electronic states in the resonant inelastic X-ray scattering process.

As they are expressed here, eqs 1 and 2 indicate that calculation of the angular anisotropy in the RIXS spectrum requires knowledge about both the transition moment from the electronic ground state to a core-excited state in the X-ray absorption spectrum and the transition moment from the core-excited state to a valence-excited state. In the RIXS spectra, the emission transitions are given different weights depending on the excitation energy due to the symmetries of the intermediate and final states. Because of the finite core-hole lifetime, the anisotropy is also sensitive to evolution in the core-excited state. In this study, RIXS spectra are simulated in a two-step procedure based on the calculation of the X-ray absorption and X-ray emission transitions. For isolated molecules, RIXS experiments can be modeled very accurately in a quantum dynamical treatment,[1] but these methods are not easily applicable to liquid water due to the increased complexity. The finite lifetime of the intermediate core-excited state is taken into account through real-time excited state MD simulations. The classical two-step procedure excludes the effects of both quantum dynamics and quantum interference[24,27] in the spectrum, but the classical approximation is a well-defined reference point for future improvement. Moreover, the assumption of rapid coherence loss due to intermolecular interactions in the liquid is not unreasonable. The angular anisotropy is derived from RIXS spectra at the experimental angular values of $\theta = 0°$ and $\theta = 65°$.[2]

In the present study, simulated RIXS spectra are directly derived from excited-state molecular dynamics and spectral data reported in a previous theoretical study on the fine-structure in the nonresonant XE spectrum of liquid water.[11] The X-ray emission is calculated for each of the sampled water molecules reported in the previously performed ab initio (Car−Parrinello) MD simulation[11,28,29] of liquid water. The transition moments required to determine the X-ray emission are calculated along the trajectory of the core-excited state dynamics and are weighted according to an exponential core-hole decay.[5,11,22] The XE transition moments are derived from electronic ground state calculations, excluding of the core-excited electron.

The X-ray absorption is calculated at the ground state geometry, initial to the core-excited state dynamics. The various possible approximations[14,15,17] used to simulate the XA spectrum in liquid water yield different interpretations. Here I compare the performance of the half core-hole approximation (HCH), the full core-hole approximation (FCH), and an approximation in which the calculation of the entire XA spectrum is based on the lowest core-excited state (XCH).[14,15,17] In the modeling of the RIXS process, I have employed the HCH approximation that has been proven to have the best overall performance in its description of the XA spectrum of liquid water. The XA spectra are simulated with the StoBe code[30] using the same computational framework as in previous publications.[31] In particular, the energy scale of the entire XA spectrum is corrected in a ΔKohn−Sham approximation[31,32] to the lowest core-excited state. On the basis of a complete experimental set of RIXS data, it would be valuable to compare these data to RIXS simulations derived from other XA approximations.

To allow comparison to the experimentally determined angular anisotropy in RIXS spectra of liquid water,[2] the simulated absorption and emission spectra are convoluted using a Gaussian broadening with 1.0 and 0.4 eV full-width half-maximum, respectively.

In reality, each excitation energy corresponds to the evolution of the system on different core-excited state potentials as well as nonadiabatic processes, but in the present study I have had to approximately model this evolution. The spectrum from resonant excitations into the XA pre-edge feature at 534.5 eV is modeled by structures from a trajectory of molecular dynamics in the lowest core-hole excited state.[11] The inclusion of the core-excited electron in the dynamics is necessary since the localization is long-lived (>20 fs) for pre-edge excitations[33] and since it also strongly influences the excited-state dynamics.[5] The

evolution in core-excited states above 538 eV is approximated by trajectories from MD simulations in the core-ionized state,[11] since ultrafast electron delocalization (<1 fs) is observed for excitations into the XA main- and postedge.[33]

3. Results

Ab initio simulations of RIXS spectra require a faithful representation of both X-ray absorption and X-ray emission together with the response in the intermediate core-excited state. I have employed a two-step "ansatz" involving separate calculations of the processes of X-ray absorption and X-ray emission and a classical approximation to the intermediate core-excited state evolution. Before showing the results from the investigation into the angular dependence, the methodological choices behind the approximations in the simulations are explicitly stated and XA and XE spectra are also presented.

To allow a meaningful discussion, the XA and XE spectra are decomposed into their the symmetry components. The coordinate system of the initially intact water molecule is used to define the principal axis, as was first implemented in ref 11. The gas phase C_{2v} symmetry classes are just used just to denote the directions despite the fact that molecular symmetry is broken both by the environment and the excited state dynamics.

3.1. X-ray Emission. Employing electronic structure calculations to model X-ray emission spectra is a well-established tool,[34,35] but for the purpose of sampling over initial conditions and core-hole lifetimes, the relative energy scale needs to be known to high accuracy. In order to improve accuracy for comparison to high-resolution experimental data, a ΔKohn−Sham correction to the XE spectra is employed.[11] An explicit calculation of the intermediate and final states involved in the emission from the out-of-plane lone-pair $1b_1$ state is used to determine the energy scale of the entire XE spectrum.[11] An additional energy shift of −0.7 eV was included as previously determined[11] for resonant XE spectra to account for the influence of the core-excited electron. Calculated XE spectra, which are lifetime averages of XE spectra along the excited state dynamics trajectories reported in ref 11, for nonresonant and resonant(pre-edge) excitations are presented in Figure 1.

Although the excited-state dynamics is excitation-energy dependent and has a profound effect on the XE spectra of water,[5,11,22] it is described well with classical excited-state MD simulations. The selectivity of X-ray excitations in the XA pre-edge to configurations with a large asymmetry in the donating H-bonds[13,31] is also taken into account but the nonresonant XE spectrum is not very sensitive to the H-bond environment.[11] The resulting spectral differences arise primarily from different dynamical responses in the core-ionized and the lowest core-excited state.[11] Because of the limitations of the classical approximation, the agreement with the experimental XE spectra is only qualitative, but the essential features in the spectra are reproduced. The width of the bonding $1b_2$ state is related to the internal OH bond distribution, which is too narrow in the classical approximation. The $3a_1$ state is broadened by H-bonding and is strongly perturbed by excited state dynamics. The $1b_1$ peak remains sharp since the energy of the $1b_1$ lone-pair is only weakly dependent on the intramolecular geometry and there is little mixing with the states in surrounding molecules.

The shape of the $3a_1$ states in Figure 1 is important for the explanation of the angular anisotropy. The sharpness of part of the $3a_1$ contribution, which is due to the dynamics in the core-ionized state, should be noted. The experimentally observed splitting in the lone-pair peak[6] has been the subject of an alternative interpretation in which it was taken as evidence for liquid water being a two-component mixture.[9] However, it is shown here that the second lone-pair peak can be assigned to a transient OH species arising from ultrafast photodissociation processes. The present results confirm the applicability of classical approximations to the study of RIXS and XE spectra of liquid water.[11]

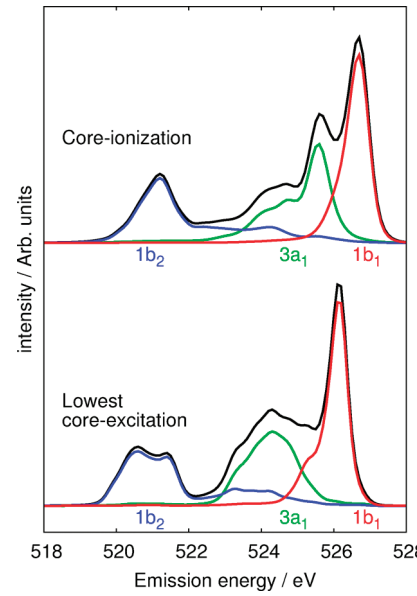

Figure 1. Spectra of X-ray emission transition moments from core-ionization (top) and the lowest core-excitation (bottom). The spectra are lifetime averages and sampled over different configurations. Overlap effects in the RIXS process are not taken into account. The total spectra are decomposed into contributions from different Cartesian directions as denoted by the b_1, a_1, and b_2 symmetry classes of the intact water molecule.

3.2. X-ray Absorption. The choice of computational method for studying the XA spectrum of liquid water is a controversial issue.[13−19,36] I have used the half core-hole (HCH) approximation[13,37,38] despite the fact that it does not reproduce the experimental XA spectrum of liquid water from the MD simulation model.[13−15,17,31,39] Simulations using the FCH and XCH approximations do show a sharp pre-edge feature, but other regions of the XA spectrum are not well reproduced.[14,15,17] The XA spectrum of liquid water is related to states which originate primarily from the in-plane O−H antibonding valence states $4a_1$ and $2b_2$ of the isolated water molecule as well as from Rydberg states. The mixing with the valence states of surrounding molecules is determined from the details of the core-hole approximation. The three methods (HCH, FCH, and XCH) all show that the pre-edge peak is predominantly of a_1 symmetry and that the states of b_2 symmetry contribute predominantly to the main- and postedge peaks. The relative contribution of a_1 and b_2 symmetries to the XA main- and postedges varies strongly with the different XA approximations and these data are shown in Figure 2. Analysis indicates that the HCH approximation has a superior overall description of the XA spectrum in the region shown in Figure 2, but it fails to reproduce the sharp pre-edge and the relative intensities in the main- and postedge regions in the experiment.[13,40] The limited success of the HCH approximation using the current ab initio MD simulation model is due to the limitations in either the spectrum calculations or the MD simulations. However, in the current situation, the relative intensities in the symmetry

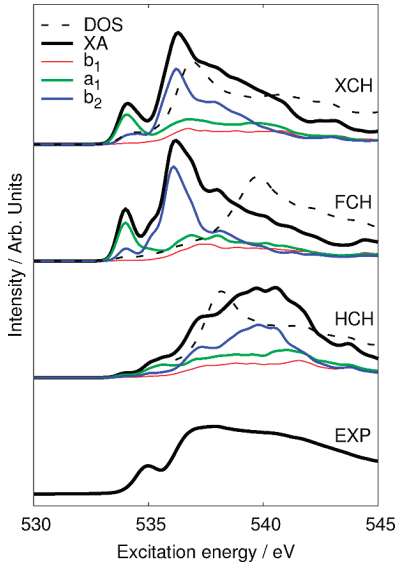

Figure 2. Average X-ray absorption spectra sampled over the simulation model used in ref 11. Results for the HCH, FCH, and XCH approximations[14,15,17] are compared to the experimental spectrum.[13,40] The spectra are decomposed into symmetry classes as in Figure 1. The total density of states is also included to specify the approximate position in the conduction band.

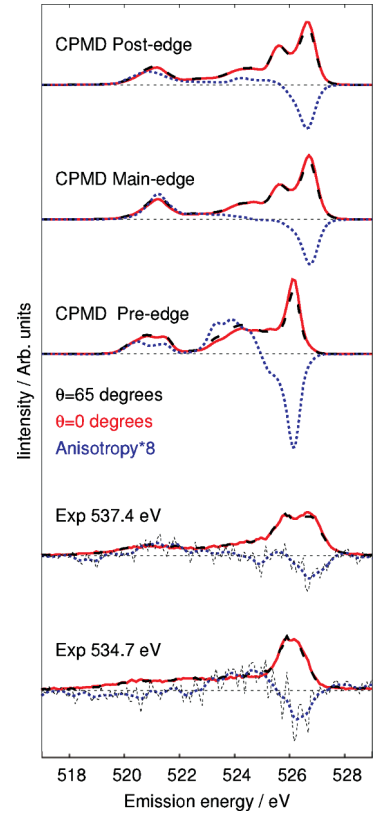

Figure 3. RIXS spectra are presented for excitation energies (535, 538, and 541 eV) representative for the pre-, main- and postedge regions in the X-ray absorption spectrum of liquid water.[13,40] Area normalized spectra are calculated for angles of 0 (in solid red lines) and 65° (in dashed black lines) between the polarization direction of the incoming light and direction from the sample to the detector. Simulated spectra are compared to experimental data from ref 2. The angular anisotropy (in dotted blue lines) is defined as the difference between area normalized RIXS spectra and is multiplied by a factor 8. The experimental angular anisotropy data is very noisy and therefore curves convoluted with a Gaussian broadening (0.4 eV full-maximum half-width) are inserted to guide the eye.

decomposition mainly influence the final RIXS spectra and so I employ HCH transition moments in modeling of the RIXS spectra.

3.3. Resonant Inelastic Soft X-ray Scattering. To understand the resonant inelastic soft X-ray scattering of liquid water,[2] it is crucial to include both the spectral differences in XE due to the dynamics illustrated in Figure 1 and the orientational information depending on the nature of the core-excited states in the XA spectrum which is shown in Figure 2. The dependence of the anisotropy on the excitation energy directly involve these effects, and in addition the selective nature of the core-excitations to particular structural configurations will also contribute.

RIXS spectra are simulated based on the initial XA transition moments and the sampling of XE transition moments from the relevant trajectories of the core-excited state dynamics. This two-step procedure follows naturally from the classical molecular dynamics approximation.[24,27]

The RIXS process is strongly influenced by ultrafast electron dynamics that can be studied by resonant photo emission spectroscopy (RPES).[33] At energies around 540 eV, there is ultrafast electron delocalization (<1 fs) in the XA spectrum whereas for pre-edge excitation the excited electron stays localized for >20 fs.[33] The degree of electron delocalization is determined by nonadiabatic processes that are influenced by the onset of the conduction band. The position of the conduction band can also be derived from theory but the uncertainty is large as since it varies strongly with the computational approximations shown in Figure 2. The total density of states shown in Figure 2 is at similar energies for the HCH and XCH approximations but is very different for FCH despite the similarities in the XA spectra for FCH and XCH.

The RPES results imply that the core-ionized state should be an excellent representation of the dynamics occurring in the core-excited states in the higher region of the XA spectrum. Therefore, the nonresonant XE spectra from core-ionization are used to calculate RIXS spectra in the main- and postedge regions. The selectivity to particular configurations is not taken into account when modeling the excitation-energy dependence above 538 eV. Instead, the pre-edge RIXS spectra are calculated from simulations in which the core-excited electron is explicitly included in the dynamics. Since a resonant pre-edge excitation also preferentially selects configurations with high pre-edge intensity in the XA spectrum, only a small subclass of water configurations are effectively probed.

The data for the angular anisotropy plotted in Figure 3 are derived from the difference of area-normalized spectra, in contrast with the equivalent presentation made in ref 2. The choice of area-normalization makes the interpretation more transparent since analysis of the data plotted in Figure 2 shows that most regions in the XA spectrum contain contributions from core-excited states of more than one symmetry. Considering the uncertainties in the XA spectrum calculations, it is not meaningful to present simulated RIXS spectra for the precise experimental energies.[2] Instead, RIXS spectra are calculated for energies representative for pre-, main- and postedge excitations.

Regardless of the excitation energy, the angular anisotropy in RIXS shown in Figure 3 is clearly negative for the b_1 states. This is consistent with the observation from the data shown in Figure 2 that the b_1 component does not dominate anywhere in the XA spectrum. For resonant pre-edge excitations (with intermediate states predominantly of a_1 character), the anisotropy is positive for the a_1 occupied states. In contrast to experiment,

the anisotropy is also slightly positive for the b_2 states. The angular anisotropy in the main-edge RIXS spectrum is positive for b_2 states and negative for a_1 states since in this region of the XA spectrum there are core-excitations of enhanced b_2 character and reduced a_1 character. In the calculations, there are small but interesting differences between the anisotropy in RIXS for main-edge and postedge excitations.

The calculated angular anisotropy shown in Figure 3 is in reasonable agreement with the experimental data[2] at both available excitation energies. For pre-edge excitations, the sign in the region of the b_2 states is not reproduced, which could mean that the relative contribution of b_2 character to the pre-edge in the calculated spectra is overestimated in the HCH approximation. The contribution from b_2 symmetry to the XA pre-edge differs in the HCH, FCH, and XCH approximations, as illustrated in Figure 2. Taken together, these observations are indicative of the crucial role of the core-hole model for a correct representation of the mixing of electronic states. An important aspect of the simulated spectra is that the shape of angular anisotropy in the a_1 region in the RIXS spectra is reproduced both for pre-edge and main-edge excitations. This confirms that the computational framework is accurate enough to claim that the fine-structure in X-ray emission is due to core-hole excited state dynamics and that the classical approximation is qualitatively valid.

4. Discussion

From the combined experimental and theoretical evidence,[13−15,17,31] it is known that the configurational selectivity at different XA excitation energies has to be taken into account in the modeling of the RIXS of liquid water. Previously, it has been shown using the HCH approximation to the XA spectrum of liquid water[31] that there is a strong sensitivity in the XA spectrum to both the H-bond length and also the asymmetry in the H-bonding around the water molecules in liquid water. In the FCH and XCH approximations,[14,15,17] the response is weaker but exhibits similar trends as in the HCH approximation. At the XA pre-edge, water molecules, which are primarily in asymmetric H-bond configurations, are probed, while at the XA postedge contributions from tetrahedrally coordinated water molecules with strong H-bonds dominate. In the intermediate energy range around the XA main-edge, water molecules with weak H-bonding also contribute. According to the calculations, there is less structural information in the XE spectra of liquid water than in XA spectroscopy since different H-bond coordination classes show similar electronic structure of the occupied orbitals. The explanation for the different response in the occupied states is that the unoccupied states probed in XA spectroscopy are more extended and exhibit a larger overlap with the surroundings.

In addition to the selective nature of the core-excitations, RIXS spectra contain information on both the particular symmetry of the core-excited state as well as the excited-state dynamics occurring during the finite core-hole lifetime.[5,11] To conclude, RIXS spectroscopy can be used to extract structural information but the information is deeply buried due to the dynamical response in the intermediate core-excited state. However, the RIXS process can be used to unravel the nature of the XA spectrum of liquid water.

In the treatment employed in this paper, although the most important effects in the RIXS process are taken into account, quantum effects are neglected.[24,27] The present approach captures the essential features of the angular anisotropy in the experimental RIXS spectra.[2] A quantitative simulation of the RIXS spectrum of liquid water would require both computationally extremely demanding as well as conceptually difficult simulations. However, it is also important to state what would need to be improved.

(A) The quantum nature of the hydrogen atoms in water should be described in both the ground- and core-excited states. In this paper, I resort to the classical approximation.

(B) Instead of choosing one (HCH) out of many different approximations for the XA spectrum calculations,[13−15,17] it would be preferable to find a highly accurate and noncontroversial method that is compatible with a well-established structural model. However, that is not presently possible. Details in the XA spectrum are influenced both by the selectivity and the symmetry of the core-excited states at each excitation energy.

(C) Methods to follow the excited-state dynamics in a manifold of electronic states would allow for the explicit energy-dependence of the excited-state dynamics to be investigated. The analysis described here is based on only two principally different forms of dynamics (from trajectories in the lowest core-excited and core-ionized states).

(D) Finally on the basis of quantum mechanical methods, the two-step approximation to the simulation of the RIXS spectrum could be avoided and quantum interference effects addressed.[24,27]

5. Conclusions

From the present study, I conclude on the basis of the XE and XA spectra derived from ab initio MD simulations on liquid water[5,11,22] that the angular anisotropy in RIXS spectroscopy[2] is compatible with an interpretation of the fine-structure in the high-resolution XE spectrum[6,7] in terms of dynamical response. The spectral signature of a transient OH species is consistent with both XE and RIXS data.

The experimentally observed differences in the angular dependence between the RIXS spectra from pre-edge and main-edge excitations are reasonable well reproduced. This is direct evidence of the excitation-energy dependence in the nuclear dynamics in the core-excited states. The simulations explain why the two lone-pair peaks are of different symmetry. Thus, there is is no motivation to abandon the MD simulation models in favor of the two-component mixture models of liquid water[9] on the basis of the data from XE spectroscopy, However, one must also realize that the XE data does not contradict the two-component model, since the structural information content is limited by dynamical effects.

The large dynamical response observed for water is due to the small weight of the hydrogen atoms. Therefore, similar effects will be present in the XE spectra of other H-bonded liquids. Strong perturbations by core-excitations can induce strong forces in any core-excited molecule and depending on inertia and lifetime of the core-excited state, similar effects will be also important in other systems.

The simulations indicate that further experimental RIXS studies with an improved signal-to-noisy ratio and which cover a wider range of energies in the near-edge X-ray absorption spectrum will provide valuable information in the ongoing debate on the interpretation of the XA spectrum of liquid water. Bulk ice is an important reference system for RIXS spectroscopy, since the main-edge feature is isotropic according to the XA (HCH) calculations. The RIXS spectra of surface adsorbates or the surface of ice would contain information on the orientation of the water molecules at the interface.[34,35]

The most important issue in the simulation of the XA spectrum of liquid water is to obtain an accurate model of the core-excitations and a balanced description of the mixing of antibonding valence states (arising from the pure $4a_1$ and $2b_2$ states in the isolated water molecule) and Rydberg states from the core-excited water molecules and their surrounding. Analysis of the data plotted in Figure 2 indicated that the localization of unoccupied states due to the presence of the core-hole is modeled very differently in the various approximations.[14,15,17,31,32] Mixing of states directly influences the spectral response of the system to structural distortions in the H-bond network. Therefore, the information from RIXS spectroscopy will help in the evaluation and development of computation methods for calculating oxygen K-edge XA spectra of water.

Acknowledgment. The present study was possible through generous allocations of computer time at the Swedish National Supercomputer Center (NSC) and Center for Parallel Computing (PDC), Sweden. The work was supported by the Swedish Research Council (VR). The XCH implementation in the StoBe code was done by LGM Pettersson. I gratefully acknowledge Johan Forsberg and Jan-Erik Rubensson for interesting discussions and for giving me direct access to the experimental data.

References and Notes

(1) *Soft X-ray Emission Spectroscopy*; Kurmaev, E., Nordgren, J., Eds.; Elsevier: Amsterdam, 2000; Vol *110*−*111*, pp 1−363.
(2) Forsberg, J.; Gråsjö, J.; Brena, B.; Nordgren, J.; Duda, L.-C.; Rubensson, J.-E. *Phys. Rev. B* **2009**, *79*, 132203.
(3) Kashtanov, S.; Augustsson, A.; Luo, Y.; Guo, J.-H.; Såthe, C.; Rubensson, J.-E.; Siegbahn, H.; Nordgren, J.; Ågren, H. *Phys. Rev. B* **2004**, *69*, 024201.
(4) Guo, J.-H.; Luo, Y.; Augustsson, A.; Rubensson, J.-E.; Såthe, C.; Ågren, H.; Siegbahn, H.; Nordgren, J. *Phys. Rev. Lett.* **2002**, *89*, 137402.
(5) Odelius, M.; Ogasawara, H.; Nordlund, D.; Fuchs, O.; Weinhardt, L.; Maier, F.; Umbach, E.; Heske, C.; Zubavichus, Y.; Grunze, M.; Denlinger, J. D.; Pettersson, L. G. M.; Nilsson, A. *Phys. Rev. Lett.* **2005**, *94*, 227401.
(6) Fuchs, O.; Maier, F.; Weinhardt, L.; Weigand, M.; Blum, M.; Zharnikov, M.; Denlinger, J.; Grunze, M.; Heske, C.; Umbach, E. *Nucl. Instrum. Methods Phys. Res., Sect. A* **2008**, *585*, 172–177.
(7) Fuchs, O.; Zharnikov, M.; Weinhardt, L.; Blum, M.; Weigand, M.; Zubavichus, Y.; Bar, M.; Maier, F.; Denlinger, J. D.; Heske, C.; Grunze, M.; Umbach, E. *Phys. Rev. Lett.* **2008**, *100*, 027801.
(8) Fuchs, O.; Zharnikov, M.; Weinhardt, L.; Blum, M.; Weigand, M.; Zubavichus, Y.; Bär, M.; Maier, F.; Denlinger, J. D.; Heske, C.; Grunze, M.; Umbach, E. *Phys. Rev. Lett.* **2008**, *100*, 249802.
(9) Tokushima, T.; Harada, Y.; Takahashi, O.; Senba, Y.; Ohashi, H.; Pettersson, L. G. M.; Nilsson, A.; Shin, S. *Chem. Phys. Lett.* **2008**, *460*, 387.
(10) Pettersson, L. G. M.; Tokushima, T.; Harada, Y.; Takahashi, O.; Shin, S.; Nilsson, A. *Phys. Rev. Lett.* **2008**, *100*, 249801.
(11) Odelius, M. *Phys. Rev. B* **2009**, *79*, 144204.
(12) Myneni, S.; Luo, Y.; Näslund, L.-Å.; Cavalleri, M.; Ojamäe, L.; Ogasawara, H.; Pelmenschikov, A.; Wernet, P.; Väterlein, P.; Heske, C.; Hussain, Z.; Pettersson, L. G. M.; Nilsson, A. *J. Phys. Cond. Matt.* **2002**, *14*, L213–L219.
(13) Wernet, P.; Nordlund, D.; Bergmann, U.; Cavalleri, M.; Odelius, M.; Ogasawara, H.; Näaslund, L.-Å.; Hirsch, T. K.; Ojamäe, L.; Glatzel, P.; Pettersson, L. G. M.; Nilsson, A. *Science* **2004**, *304*, 995–999.
(14) Hetenyi, B.; Angelis, F. D.; Gianozzi, P.; Car, R. *J. Chem. Phys.* **2004**, *120*, 8632–8637.
(15) Prendergast, D.; Galli, G. *Phys. Rev. Lett.* **2006**, *96*, 215502.
(16) Smith, J. D.; Cappa, C. D.; Wilson, K. R.; Messer, B. M.; Cohen, R. C.; Saykally, R. J. *Science* **2004**, *306*, 851–853.
(17) Cavalleri, M.; Odelius, M.; Nordlund, D.; Nilsson, A.; Pettersson, L. G. M. *Phys. Chem. Chem. Phys.* **2005**, *7*, 2854–2858.
(18) Cappa, C. D.; Smith, J. D.; Wilson, K. R.; Saykally, R. J. *J. Phys.: Cond. Matt.* **2008**, *20*, 205105.
(19) Smith, J. D.; Cappa, C. D.; Messer, B. M.; Drisdell, W. S.; Cohen, R. C.; Saykally, R. J. *J. Phys. Chem. B* **2006**, *110*, 20038–20045.
(20) Guo, J.-H.; Luo, Y.; Augustsson, A.; Kashtanov, S.; Rubensson, J.-E.; Shuh, D. K.; Ågren, H.; Nordgren, J. *Phys. Rev. Lett.* **2003**, *91*, 157401.
(21) Kashtanov, S.; Augustson, A.; Rubensson, J.-E.; Nordgren, J.; Ågren, H.; Guo, J.-H.; Luo, Y. *Phys. Rev. B* **2005**, *71*, 104205.
(22) Brena, B.; Nordlund, D.; Odelius, M.; Ogasawara, H.; Nilsson, A.; Pettersson, L. G. M. *Phys. Rev. Lett.* **2004**, *93*, 148302.
(23) Gel'mukhanov, F.; Ågren, H. *Phys. Reports* **1999**, *312*, 87–330.
(24) Ågren, H.; Gel'mukhanov, F. *J. Electron Spectrosc. Relat. Phenom.* **2000**, *110*−*111*, 153–178.
(25) Kramers, H. A.; Heisenberg, W. *Z. Phys.* **1925**, *31*, 681–708.
(26) Gel'mukhanov, F.; Sałek, P.; Privalov, T.; Ågren, H. *Phys. Rev. A* **1999**, *59*, 380–389.
(27) Luo, Y.; Ågren, H.; Gel'mukhanov, F. *Phys. Rev. A* **1996**, *53*, 1340–1348.
(28) Car, R.; Parrinello, M. *Phys. Rev. Lett.* **1985**, *55*, 2471.
(29) 1997–2007, CPMD, Copyright IBM Corp. 1990–2004, Copyright MPI für Festkörperforschung Stuttgart 1997−2001.
(30) Hermann, K.; Pettersson, L. G. M.; Casida, M. E.; et al. *StoBe*; StoBe Software: Stockholm, Berlin, Montreal, 2002.
(31) Odelius, M.; Cavalleri, M.; Nilsson, A.; Pettersson, L. G. M. *Phys. Rev. B* **2006**, *73*, 024205.
(32) Kolczewski, C.; Püttner, R.; Plashkevych, O.; Ågren, H.; Staemmler, V.; Martins, M.; Snell, G.; Schlachter, A. S.; Sant'Anna, M.; Kaindl, G.; Pettersson, L. G. M. *J. Chem. Phys.* **2001**, *115*, 6426–6437.
(33) Nordlund, D.; Ogasawara, H.; Bluhm, H.; Takahashi, O.; Odelius, M.; Nagasono, M.; Pettersson, L. G. M.; Nilsson, A. *Phys. Rev. Lett.* **2007**, *99*, 217406.
(34) Nilsson, A. *J. Electron Spectrosc. Relat. Phenom.* **1998**, *93*, 143–152.
(35) Nilsson, A.; Pettersson, L. G. M. *Surf. Sci. Rep.* **2004**, *55*, 49–167.
(36) Nilsson, A.; Wernet, P.; Nordlund, D.; Bergmann, U.; Cavalleri, M.; Odelius, M.; Ogasawara, H.; Näslund, L.-Å.; Hirsch, T. K.; Ojamäe, L.; Glatzel, P.; Pettersson, L. G. M. *Science* **2005**, *308*, 793.
(37) Triguero, L.; Pettersson, L. G. M.; Ågren, H. *Phys. Rev. B* **1998**, *58*, 8097–8110.
(38) Slater, J. C.; Johnsson, K. H. *Phys. Rev. B* **1972**, *5*, 844.
(39) Cavalleri, M.; Odelius, M.; Nilsson, A.; Pettersson, L. G. M. *J. Chem. Phys.* **2004**, *121*, 10065–10075.
(40) Näslund, L.-Å.; Lüning, J.; Ufuktepe, Y.; Ogasawara, H.; Wernet, P.; Bergmann, U.; Pettersson, L. G. M.; Nilsson, A. *J. Phys. Chem. B* **2005**, *109*, 13835–13839.

JP903096K